

Research Article: New Research | Cognition and Behavior

## Implementing Goal-Directed Foraging Decisions of a Simpler Nervous System in Simulation

Jeffrey W. Brown<sup>1</sup>, Derek Caetano-Anollés<sup>2</sup>, Marianne Catanho<sup>3</sup>, Ekaterina Gribkova<sup>4</sup>, Nathaniel Ryckman<sup>5</sup>, Kun Tian<sup>6</sup>, Mikhail Voloshin<sup>7</sup> and Rhanor Gillette<sup>8</sup>

<sup>1</sup>University of Illinois College of Medicine at Urbana-Champaign, University of Illinois at Urbana-Champaign, Urbana, Illinois 61801

<sup>2</sup>Max-Planck-Institut Für Evolutionsbiologie, August-Thienemann-Str. 2, Plön, D-24306

<sup>3</sup>Department of Bioengineering, University of California - San Diego, La Jolla, CA 92093-0412

<sup>4</sup>Neuroscience Program, Beckman Institute, University of Illinois at Urbana-Champaign, 61801

<sup>5</sup>University Library, University of Illinois at Urbana-Champaign, 1408 W. Gregory Dr, Urbana, IL 61801

<sup>6</sup>Department of Biology, Emory University, 1510 Clifton Rd NE, Room 2172, Atlanta, GA 30322

<sup>7</sup>Mighty Data, Inc, 11 Midwood St #C9, Brooklyn, NY 11225

<sup>8</sup>Department of Molecular & Integrative Physiology, University of Illinois at Urbana-Champaign, Urbana, Illinois 61801

DOI: 10.1523/ENEURO.0400-17.2018

Received: 20 November 2017

Revised: 3 February 2018

Accepted: 6 February 2018

Published: 26 February 2018

**Author Contributions:** JWB, DC\_A, MC, EG, NR, KT, MV, and RG designed and performed research. JWB, EG, and RG wrote the paper.

**Funding:** [http://doi.org/10.13039/100000001National Science Foundation \(NSF\) IOB 04-47358](http://doi.org/10.13039/100000001National%20Science%20Foundation%20(NSF)IOB%2004-47358)

**Funding:** [http://doi.org/10.13039/100000002HHS | National Institutes of Health \(NIH\) R21 DA023445](http://doi.org/10.13039/100000002HHS%20National%20Institutes%20of%20Health%20(NIH)R21%20DA023445)

**Conflict of Interest:** Authors report no conflict of interest.

Supported in early stages by National Science Foundation grant IOB 04-47358 and National Institutes of Health grant R21 DA023445.

**Correspondence:** Rhanor Gillette, Department of Molecular & Integrative Physiology, 407 Goodwin Ave., 524 Burrill Hall, University of Illinois at Urbana-Champaign Urbana, IL 61801. Email: [rhanor@illinois.edu](mailto:rhanor@illinois.edu)

**Cite as:** eNeuro 2018; 10.1523/ENEURO.0400-17.2018

**Alerts:** Sign up at [eneuro.org/alerts](http://eneuro.org/alerts) to receive customized email alerts when the fully formatted version of this article is published.

Accepted manuscripts are peer-reviewed but have not been through the copyediting, formatting, or proofreading process.

Copyright © 2018 Brown et al.

This is an open-access article distributed under the terms of the Creative Commons Attribution 4.0 International license, which permits unrestricted use, distribution and reproduction in any medium provided that the original work is properly attributed.

**Title:** Implementing goal-directed foraging decisions of a simpler nervous system in simulation

**Abbreviated Title:** Foraging Decision and the Simple Brain

**Authors:** Jeffrey W. Brown<sup>1</sup>, Derek Caetano-Anollés<sup>2</sup>, Marianne Catanho<sup>3</sup>, Ekaterina Gribkova<sup>4</sup>, Nathaniel Ryckman<sup>5</sup>, Kun Tian<sup>6</sup>, Mikhail Voloshin<sup>7</sup>, and Rhanor Gillette<sup>8\*</sup>

**Affiliations:** <sup>1</sup> University of Illinois College of Medicine at Urbana-Champaign, University of Illinois at Urbana-Champaign, Urbana, Illinois 61801

<sup>2</sup> Max-Planck-Institut für Evolutionsbiologie, August-Thienemann-Str. 2, D-24306 Plön

<sup>3</sup> Department of Bioengineering, University of California - San Diego, La Jolla, CA 92093-0412

<sup>4</sup> Neuroscience Program, Beckman Institute, University of Illinois at Urbana-Champaign, 61801

<sup>5</sup> University Library, University of Illinois at Urbana-Champaign, 1408 W. Gregory Dr. | Urbana, IL 61801

<sup>6</sup> Dept. Biology, 1510 Clifton Rd NE, Room 2172, Emory University, Atlanta, GA, 30322

<sup>7</sup> Mighty Data, Inc., 11 Midwood St #C9, Brooklyn, NY 11225

<sup>8</sup> Dept. Molecular & Integrative Physiology, University of Illinois at Urbana-Champaign, Urbana, Illinois 61801

**Author Contributions:** JWB, DC\_A, MC, EG, NR, KT, MV, and RG designed and performed research. JWB, EG, and RG wrote the paper.

**Correspondence:** Rhanor Gillette, Department of Molecular & Integrative Physiology, 407 Goodwin Ave., 524 Burrill Hall, University of Illinois at Urbana-Champaign Urbana, IL 61801  
Email: [rhanor@illinois.edu](mailto:rhanor@illinois.edu)

**Figures:** 4;

**Tables:** 0

**Abstract:** 162 words

**Significance Statement:** 114 words

**Multimedia:** 0

**Introduction:** 420 words

**Discussion:** 1145 words

**Acknowledgements:** Mikhail Voloshin implemented a first Cyberslug version in this lab in 1999, programming in C++ and using a perceptron learning mechanism. We thank Mark Nelson (UIUC) for introduction to NetLogo. We recognize intellectual and collegial contributions of the Microsoft Research/University of Washington Summer Institutes on Intelligent Systems.

**Conflict of Interest:** Authors report no conflict of interest

**Funding Sources:** Supported in early stages by National Science Foundation grant IOB 04-47358 and National Institutes of Health grant R21 DA023445.

**Implementing goal-directed foraging decisions  
of a simpler nervous system in simulation**

1  
2  
3  
4  
5  
6  
7  
8  
9  
10  
11  
12  
13  
14  
15  
16  
17  
18  
19  
20  
21

**Abstract**

Economic decisions arise from evaluation of alternative actions in contexts of motivation and memory. In the predatory sea-slug *Pleurobranchaea* the economic decisions of foraging are found to occur by the workings of a simple, affectively controlled homeostat with learning abilities. Here, the neuronal circuit relations for approach-avoidance choice of *Pleurobranchaea* are expressed and tested in the foraging simulation Cyberslug™. Choice is organized around appetitive state as a moment-to-moment integration of sensation, motivation (satiation/hunger), and memory. Appetitive state controls a switch for approach vs. avoidance turn responses to sensation. Sensory stimuli are separately integrated for incentive value into appetitive state, and for prey location (stimulus place) into mapping motor response. Learning interacts with satiation to regulate prey choice affectively. The virtual predator realistically reproduces the decisions of the real one in varying circumstances and satisfies optimal foraging criteria. The basic relations are open to experimental embellishment toward enhanced neural and behavioral complexity in simulation, as was the ancestral bilaterian nervous system in evolution.

22 **Significance Statement:**

23 Contemporary artificial intelligence lacks the attributes of natural intelligence, in  
24 particular the abilities to relate information affectively. Accordingly, it is notable that the most  
25 complex animal behaviors serve primitive homeostatic goals, and emerge from the primitive  
26 mechanisms generating motivation and reward learning. Here is shown in simulation the  
27 function of a basic neuronal circuit for cost-benefit decision, derived from studies of a predatory  
28 generalist, the sea-slug *Pleurobranchaea*, and based on affective integration of information. Its  
29 simplicity may reflect distant ancestral qualities on which complexities in economic, cognitive,  
30 and social behaviors were built. The simulation validates experimental data and provides a basic  
31 module on which complexity in economic, cognitive, and social behaviors could be built.

32

### 33 **Introduction**

34 Foraging behavior in tracking and consuming resources is a series of economic decisions  
35 guided by stimulus characters predictive of risk and resource value. The basic behavioral choice  
36 is between an approach or avoidance of salient stimuli, a cost-benefit calculation done through  
37 integrating stimulus properties with motivation and memory. However, the natural intelligence  
38 displayed by even the simplest foraging animals has remained to be captured fully in artificial  
39 intelligence constructs in terms of actual neural computations made by real animal foragers.

40 We undertook to implement and test a model of foraging decision derived from the  
41 neuronal circuitry underlying approach-avoidance decisions in the predatory sea-slug  
42 *Pleurobranchaea*. The neuronal circuitry of decision has been characterized down to the single-  
43 neuron level (Gillette et al., 1982; London and Gillette, 1986; Jing and Gillette, 2000, 2003;  
44 Hirayama and Gillette, 2012; Hirayama et al., 2012; Hirayama et al., 2014). In particular, a key  
45 decision mechanism was found to lie in regulation of the turn motor network by the feeding  
46 network, whose excitation state depends on sensory input, memory, and satiation. Sufficient  
47 excitation in the feeding network converts default avoidance responses to sensory stimuli to  
48 approaching turns (Hirayama and Gillette, 2012). These findings localized motivation, appetitive  
49 state, and control of motor decision to the feeding network. They also account for behavior in  
50 which 1) quite hungry specimens not only orient to and bite at weak appetitive stimuli, but will  
51 also attack moderately noxious stimuli, 2) appetitive thresholds for approaching turns rise  
52 proportionately with satiation, and 3) as satiation increases, the animals avoid increasingly strong  
53 appetitive stimuli (Gillette et al., 2000; Nohoa and Gillette 2013). Further, motor choice in  
54 *Pleurobranchaea*'s learned discrimination of odors paired with unconditioned stimuli is also  
55 mediated at the feeding motor network level (Davis et al., 1980; Mpitsos and Cohan, 1986;

56 Noboa and Gillette, 2013). These relations indicate a simple neural model for cost-benefit based  
57 decision in the animal's foraging (Gillette et al., 2000; Hirayama et al., 2012).

58         The simulation Cyberslug™ implements the integrated model in an autonomous agent  
59 with behavior designed from neurophysiological and behavioral data. To our knowledge no  
60 other such empirically driven neuroeconomic simulation has yet been devised. The success and  
61 utility of Cyberslug are supported through its accurate and dynamic reproduction of functional  
62 relations in *Pleurobranchaea*'s nervous system and behavioral repertory, its ability to maintain  
63 the fitness (here, nutritional state) of a virtual predator through plausible choices of differently  
64 valued prey based on hunger state, sensation, and memory; and its capacity to weigh risk against  
65 resource value to optimize foraging decisions.

66

## 67 **Methods**

### 68 **Software Accessibility**

69         Cyberslug™ is freely available as extended data online at  
70 <https://github.com/Entience/Cyberslug>.

71

### 72 **General design of biological relations**

73         Sigmoidal relations are used as constructive approximations to simulate biological  
74 processes that accelerate from small beginnings to saturate at high values. They or their  
75 influential values appear in Equations 3.0, 5.1, 6.0, 7.1, and 7.2 to compute virtual place codes  
76 for sensory stimuli, appetitive stimulus affect, satiation, appetitive state, a behavioral switch  
77 based on appetitive state, and the amplitude of a turning response, respectively. Centers and  
78 asymptotes may be graphed for the interested reader from the values given in the source code.

79 **Learning**

80 Reward and punishment associations are formed with the prey sensory signatures,  
81 *odor\_hermi* and *odor\_flab*, using the Rescorla-Wagner algorithm for classical conditioning  
82 (Rasmussen et al., 2015):

83

84 
$$\Delta V = \alpha * \beta(\lambda - V) . \tag{1}$$

85 On a given trial the change  $\Delta V$  in the predictive value of a stimulus  $V$  (the amount of  
86 learning) depends on the difference between the value of what actually happens,  $\lambda$ , and what is  
87 expected (or already learned),  $V$ . The  $\alpha$  term is the salience constant (the attention-getting  
88 capacity) of the conditioned stimulus (CS; ranging from 0 to 1, and set here at 0.5 for both  
89 *odor\_hermi* and *odor\_flab*). The  $\beta$  term is a rate parameter for the associative capacity of the  
90 unconditioned stimulus (US) with the CS (ranging from 0 to 1; here a maximum of 1). The  $\lambda$   
91 term is the maximum associative value of the US (set at 1 for *odor\_hermi* and *odor\_flab*). The  
92 Rescorla-Wagner algorithm was selected for its intuitive layout, simplicity, and robustness in a  
93 range of learning applications (Danks, 2003; Rasmussen et al., 2015). It is a useful  
94 approximation of learning from insects to mammals (Miller et al., 1995).

95

96 **Sensory transduction and integration**

97 The Cyberslug agent uses bilaterally paired, anterior odor sensors, simplifying the real  
98 animal's chemotactile oral veil's function in prey tracking (Yafremava et al., 2007). The sensors  
99 report strengths of the three odors at slightly less than half a body length in front of the agent and  
100 at a roughly 40° angle with respect to its anteroposterior axis. For example, in the case of  
101 *betaine*, the averaged odor strength is

102

103

104 
$$sns\_betaine = \frac{sns\_betaine\_left + sns\_betaine\_right}{2} , \quad (2)$$

105

106 where  $sns\_betaine\_left$  and  $sns\_betaine\_right$  are logarithmic functions of  $betaine$  virtual  
107 concentrations at each sensor. The  $sns\_betaine$  variable integrates into the appetitive stimulus  
108 effect (Eq. 4.2).

109 The *Somatic\_Map* function transforms sensory input into a virtual place code of the  
110 estimated direction of the strongest odor. It includes a mechanism emphasizing the salience of  
111 the nearest prey, analogous to surround suppression mechanisms underlying attention (Boehler et  
112 al., 2008): when closer to one prey type, sensation of the other is decreased, which reduces  
113 consumption of the aversively learned Flab in the presence of the odor of Hermi. The output of  
114 *Somatic\_Map* is a template for the turn amplitudes of resulting approach-avoidance responses:

115

116 
$$Somatic\_Map = \left( \frac{sns\_flab\_left - sns\_flab\_right}{1 + e^{-k0 \cdot F}} + \frac{sns\_hermi\_left - sns\_hermi\_right}{1 + e^{-k0 \cdot H}} \right)$$
  
117 (3.1)

118 where

119 
$$F = sns\_flab - sns\_hermi$$
  
120 (3.2)

121 and

122 
$$H = sns\_hermi - sns\_flab .$$
  
123 (3.3)



124

125           The Incentive variable (*Incentive*) integrates sensory information of positive and negative  
126 valences. It represents the incentive potential of a stimulus as modulated by learning and  
127 motivation:

128

$$129 \qquad \qquad \qquad \text{Incentive} = R^+ - R^- \quad , \qquad \qquad \qquad (4.1)$$

130

131 where  $R^+$  and  $R^-$  represent appetitive and aversive stimulus affects, respectively:

132

133

$$134 \qquad \qquad \qquad R^+ = \frac{\text{sns\_betaine}}{1 + k1 \cdot V_h \cdot \text{sns\_hermi}} + k3 \cdot V_h \cdot \text{sns\_hermi} \quad . \qquad \qquad \qquad (4.2)$$

135

136  $R^+$  encodes the odor intensity of the primary resource indicator, betaine, in the first term. The  
137 positive association of Hermi odor becomes prominent with learning in the second term, and  
138 betaine values become less prominent. The variable  $R^-$  represents the learned negative  
139 association of Flab odor. This variable might also encode negative effects of pain pathways, but  
140 in the present formulation it omits explicit pain and simply treats its consequences on aversive  
141 learning.

142

$$143 \qquad \qquad \qquad R^- = k3 \cdot V_f \cdot \text{sns\_flab} \qquad \qquad \qquad (4.3)$$

144

145

146 **Satiation and appetitive state**

147 Hunger state is represented through the function *Satiation*, which reflects *Nutrition* in a  
 148 sigmoid relation with a lower bound near 0 and an upper asymptote at 1:

149

$$150 \quad \text{Satiation} = \frac{1}{\left(1 + k4 \cdot e^{-4 \cdot \text{Nutrition} + 2}\right)^2}, \quad (5.1)$$

151

152 where *Nutrition*, without prey consumption, decreases recursively with each time step:

153

$$154 \quad \text{Nutrition}_{t+1} = \text{Nutrition}_t - 0.0005 \cdot \text{Nutrition}_t. \quad (5.2)$$

155

156 When feeding occurs, *Nutrition* is increased by a value of 0.3. The simulation initializes with  
 157 *Nutrition* set at 0.8.

158

159 Appetitive state (*App\_State*) is a function of *Incentive* and *Satiation*. It defines the  
 160 thresholds for decisions to approach or avoid given prey items. It parallels expression of  
 161 appetitive state in the excitation of *Pleurobranchaea*'s feeding network (Hirayama and Gillette,  
 162 2012). The sigmoidal element increases *App\_State* as *Incentive* increases, and decreases it as  
 163 *Satiation* increases. As in the real animal, *App\_State* is transiently suppressed during avoidance  
 164 turning (Brown, Noboa and Gillette, in preparation). This acts to further bias decision away from  
 165 approach during the avoidance turn when some appetitive sensory input is present:

165

$$166 \quad \text{App\_State} = 0.01 + \frac{1}{\left(1 + e^{-k5 \cdot \text{Incentive} + k6 \cdot \text{Satiation}}\right)} + k7 \cdot (\text{App\_State\_Switch} - 1), \quad (6.0)$$

167

168 where the expression ( $App\_State\_Switch - 1$ ), defined and discussed later, causes a transient  
 169 suppression of  $App\_State$  during avoidance turns. It may be noted that satiation state is a variable  
 170 in both *Incentive* and  $App\_State$ , which reflects findings that satiation state is expressed in the  
 171 basal excitation state of the feeding network, and that satiation may modulate sensory gain in the  
 172 periphery (unpublished).

173 The *Satiation* term dominates  $App\_State$  values at its extreme ranges (0 and 1). *Incentive*  
 174 is significant in the mid-range, as in *Pleurobranchaea* (Gillette et al., 2000). When *Satiation* is  
 175 either very low or high, it dominates over the *Incentive* term. When very low, the Cyberslug  
 176 agent chooses to consume the previously learned, noxious Flab. When very high, it actively  
 177 avoids otherwise appetitive Hermis. These choices reproduce those made by very satiated or  
 178 hungry *Pleurobranchaea* (Gillette et al., 2000; Noboa and Gillette, 2013).

179

### 180 **Turning and locomotion**

181 The function  $App\_State\_Switch$  switches the turn motor network from avoidance to  
 182 approach, representing the  $ASw_{1,2}$  actions of Figure 2. It acts like the corollary outputs from  
 183 *Pleurobranchaea*'s feeding network that toggle the turn motor network polarity (Brown, 2014).  
 184 The function converges steeply to either 1 or -1 depending on the value of  $App\_State$ :

185

186

$$187 \quad App\_State\_Switch = \frac{-2}{1 + e^{-k8 \cdot (App\_State - 0.245)}} + 1, \quad (7.1)$$

188

189 In particular, when *App\_State* goes below or above a threshold, set here as 0.245,  
 190 *App\_State\_Switch* approaches 1 or -1, respectively, to govern turn direction. This threshold  
 191 might well be a variable influenced by reproductive state, health, or neuromodulatory inputs  
 192 from other neuronal networks (cf. Hirayama and Gillette, 2014), but is set as a simple constant  
 193 here.

194

195 The turn is computed in degrees as:

196

$$197 \quad Turn\_Angle = \frac{k9 \cdot App\_State\_Switch}{1 + e^{3 \cdot Somatic\_Map}} - App\_State\_Switch, \quad (7.2)$$

198

199 where positive or negative values of *App\_State\_Switch* cause avoidance or approach turns,  
 200 respectively. Sufficient excitation in the Feeding Network (when *App\_State* is greater than  
 201 0.245) switches the polarity of an elicited turn from avoidance to approaching, while  
 202 *Somatic\_Map* determines turn magnitude by supplying somatotopic information on stimulus  
 203 location.

204 When not actively engaged in prey approach or avoidance, the Cyberslug agent pursues a  
 205 wandering trajectory, given as

206

$$207 \quad Turn\_Angle = -1 + random\_float(2) \quad (7.3)$$

208

209 The *random\_float* function generates a floating-point number between 0 and 2. In this case it  
 210 causes random changes in heading ranging from -1 to 1 degree on each time step.

211

212

## 213 **Results**

### 214 **The core model**

215           Cyberslug is based on neuronal relations of approach-avoidance decision in  
216 *Pleurobranchaea*'s responses to odors of potential prey (Gillette et al., 2000; Hirayama and  
217 Gillette, 2012). Figure 1 shows the flow of information, from initial feature extraction of  
218 different sensory inputs to their evaluation in terms of estimated total resource value (Incentive),  
219 based on nutritional need and memory; these processes then direct motor output for approach or  
220 avoidance turns. Figure 2 shows the logic of the model's implementation into Cyberslug. The  
221 relations are represented in simple equations that drive the agent. Values of the constants ( $K_n$ ) in  
222 the equations were optimized over numerous trials and are found in the NetLogo code available  
223 as extended data. Altering the values in the code may lend appreciation for the role of natural  
224 selection in adaptively tuning neural circuitry.

225

226           Foraging decision is controlled by appetitive state. The animal's feeding motor network  
227 is at the core of the decision module. Its excitation state directs choice between approach and  
228 avoidance turns (Hirayama and Gillette, 2012). The excitation state manifests the appetitive state  
229 of the animal; i.e., the disposition to engage in goal-directed appetitive behavior. Appetitive state  
230 integrates the animal's satiation state, sensation, and memory of experience (Davis and Gillette,  
231 1978; Davis et al., 1980; London and Gillette, 1986; Gillette et al., 2000; Hirayama and Gillette,  
232 2012). Satiation determines the baseline excitation state of the feeding network. Incoming  
233 sensory inputs are integrated with memory into incentive. Incentive sums with satiation in the  
234 feeding network, either increasing or decreasing appetitive state.

235 By default, when appetitive state is low, the animal's nervous system is organized so that  
236 the turn response to any sensory stimulus is avoidance. During the aversive turn appetitive state  
237 is decreased by inhibitory inputs in the feeding network [Davis and Gillette, 1978; London and  
238 Gillette, 1986; Hirayama and Gillette, 2012; Brown, 2014). Increasing appetitive state inverts the  
239 turn response direction to one of approach. Thus, appetitive state determines the sensory  
240 thresholds for the approach turn toward a prey and subsequent feeding responses. When high  
241 enough, corollary outputs from the feeding network appear to switch the excitatory sensory  
242 input-encoding stimulus site from one side of the turn network to the other, resulting in a turn  
243 towards the stimulus (Brown, 2014).

244 Sensory inputs here are of four kinds: 1) a resource odor signal predicting nutritional  
245 content to *Pleurobranchaea*, the amino acid betaine (Gillette et al., 2000); 2) a specific odor  
246 signature for a particular prey species (Noboa and Gillette, 2013); 3) a place code for the  
247 averaged site of sensory input to the sensors Yafremava et al., 2007; (Yafremava and Gillette,  
248 2011); and 4) nociception (pain). (1) and (2) are summed as Incentive for resource and learned  
249 positive and negative values of prey odors ( $R^+$  and  $R^-$ , respectively), which is then integrated  
250 with motivation (Satiation) as Appetitive State in the Feeding Network. The Somatic Map  
251 variable embeds (3) as a template for turn response amplitude. Positive or negative classical  
252 learning are assumed consequences of feedback from the feeding network operating in feeding or  
253 avoidance modes, respectively.

254 The Cyberslug simulation preserves the basic interactions of feeding and turn networks in  
255 the control of the turn by appetitive state and aversive suppression of the feeding network.  
256 Simplifications include: 1) for learning, explicit pain mechanisms are omitted in favor of  
257 arbitrary consequences; 2) exploratory locomotion is the default action in absence of active

258 avoidance or approach; and 3) the switch mechanism for turn direction is rendered as a sigmoidal  
259 equation.

260

### 261 **Cyberslug environment**

262 Cyberslug is implemented in the graphic modeling, agent-based programming language  
263 NetLogo 5.3.1. (Wilensky, 1999). Agent actions and odor diffusion are executed in discrete  
264 time steps by underlying code, where agents run commands in a turn-taking mechanism to  
265 simulate concurrence. At each time step the agent positions, orientations, speeds, and odor  
266 intensities in individual patches are updated with the variables that control them.

267 The interface screen (Fig. 3) displays current values of agent-associated variables and  
268 statistics. Users may override automatic agent navigation by manually controlling these agents  
269 with the mouse, specify the number of prey objects in the environment, and switch on or off a  
270 function that traces the agent's path. When the simulation is initialized, a single Cyberslug agent  
271 and the different prey are generated at random positions in the environment.

272

### 273 **Prey**

274 The Cyberslug agent encounters two virtual prey, "Hermit" and "Flab", after the sea-slugs  
275 *Hermisenda crassicornis* and *Flabellina iodinea* which *Pleurobranchaea* can encounter in the  
276 wild (Noboa and Gillette, 2013). These are shown as small orbs, colored green for Hermit and red  
277 for Flab. Each prey secretes two odors: the resource signal *betaine*, a predictor of nutritional  
278 resource (Gillette et al., 2000), and either of "*odor\_hermit*" or "*odor\_flab*." Odors diffuse over  
279 time and space as for actual diffusion. Prey move in a simple random walk. Prey numbers remain  
280 constant; when consumed, replacements appear at random positions.

281           The specific odors of Hermi and Flab become associated with preference and avoidance,  
282 respectively, through reward learning. These effects are analogous to the ready consumption of  
283 *Hermisenda* by *Pleurobranchaea*, and the rejection and aversive learning of *Flabellina* (Noboa  
284 and Gillette, 2013). A Batesian mimic, “Faux-Flab”, is included as an option. In Nature, Batesian  
285 mimics receive protection from predation by mimicking appearance or odor of noxious species,  
286 and by their presence may increase attempted predation on the noxious species. Thus, Faux-Flab  
287 has the odor of Flab and the positive rewarding qualities of Hermi. The mimic is included for the  
288 user to test its effects on predator choices.

289

#### 290 **The Cyberslug agent**

291           Reward and punishment associations are formed with the prey sensory signatures using  
292 the Rescorla-Wagner algorithm for classical conditioning (Rescorla and Wagner, 1972), allowing  
293 the predator to learn through experience. Bilaterally paired, anterior odor sensors simplify the  
294 real animal’s chemotactile oral veil’s function in prey tracking (Yafremava and Gillette, 2011) to  
295 report the strengths of odors for betaine, a predictor of nutritional value, and the prey signature  
296 odors for *Hermisenda* and *Flabellina*. The sensors also transform sensory input into a virtual  
297 place code, giving the estimated direction of the source of the strongest odor, on which motor  
298 response is patterned. The incentive of an odor is calculated as summed positive and negative  
299 valences, which are determined by the intrinsic appetitive nature (for betaine) and learning  
300 experiences for the signature odors.

301           Appetitive state is the final regulator of behavioral choice. It summates incentive with  
302 satiation, and thus integrates sensory stimulus qualities with learning and motivation. Satiation is  
303 a simple function of nutritional state, which declines over time following prey consumption.



304 Satiation dominates appetitive state at its extreme ranges (quite hungry or not); whereas stimulus  
305 incentive is significant in the mid-range. At a threshold value, appetitive state causes a  
306 directional switch between approach or avoidance in the turn response to an odor. The choices  
307 made reproduce those seen across the spectra of learning and hunger state by *Pleurobranchaea*  
308 (Gillette et al., 2000; Noboa and Gillette, 2013).

309

### 310 **Testing the simulation**

311 Cyberslug was tested for prey selectivity as modified by learning, motivational state, and  
312 their interactions. Four sets of six tests were run under conditions assessing effects of learning  
313 and satiation mechanisms on prey selection. Effects of satiation and learning on selectivity were  
314 tested in arenas containing 1) 10 Flabs and 3 Hermis, 2) 13 Flabs alone, and 3) 13 Hermis alone.  
315 Tests ran for 150,000 software time steps.

316 Results in Figure 4 show that in the 10 Flab/3 Hermi arena satiation acted to limit the  
317 numbers of prey consumed between the two satiation and two no-satiation scenarios), while  
318 enhancement of prey selectivity depended on learning and satiation acting together. Thus, in tests  
319 where both learning and satiation mechanisms were inactivated, average total prey taken was 701  
320 (SEM 6.22), of which 21.2% (SEM 0.6%) were Hermis, slightly less than their 23.1% frequency  
321 in the population. This yielded a selectivity value (total Hermis taken/total Flabs taken) of 0.27  
322 (SEM 0.01), less than the 0.30 ratio of Hermis to Flabs in the population. This effect appeared  
323 due to a greater frequency of random clustering in the denser Flab population, leading to more  
324 frequent multiple consumptions of Flabs than Hermis. When learning was activated without  
325 satiation, average total prey taken was still high at 707.8 (SEM 5.5), of which 21.2% (SEM  
326 0.6%) again were Hermis with still a low selectivity of 0.27 (SEM 0.01). Without learning,

327 satiation alone reduced average prey consumed to 119 (SEM 0.52) with 24.1% (SEM 1.2%)  
328 Hermi, and with low selectivity of 0.32 (SEM 0.02).

329

330       Acting together, learning and satiation mechanisms led to an averaged total of 91.7 (1.43  
331 SEM) prey taken, where 82.5% (SEM 1.5%) were Hermi. The selectivity coefficient of 4.96 (0.6  
332 SEM) was a more than 18-fold increase over the values obtained without learning and/or  
333 satiation.

334       When tests were made in a field of 13 Flabs alone, with both learning and satiation intact,  
335 the averaged total prey taken was 53.3 (0.33 SEM). This low but nontrivial value reflected  
336 decisions to take noxious prey in a condition of extreme hunger, and also demonstrated  
337 combined effects of learning and satiation in reducing consumption of noxious prey (not shown).  
338 When similar runs were made in a field of 13 Hermis alone, the averaged total prey taken was  
339 143.5 (0.81 SEM). The contrast of this value with the all Flab condition highlighted effects of  
340 positive vs. negative learning in prey selection, as well as effects of satiation in limiting  
341 consumption. There were significant differences in number of prey consumed across all three  
342 arenas ( $p < 0.0001$  in a one-way ANOVA; Tukey-Kramer,  $p < 0.001$ , between all three pairs).

343

344

## 345 **Discussion**

346       The Cyberslug autonomous entity bases behavioral choice and perception on interactions  
347 of motivational state and learning, like the real animal. The algorithmic integration of sensation,  
348 motivational state, and memory reproduces adaptive action selection in behavioral choice. At  
349 intermediate values of satiation, the experienced Cyberslug agent selectively prefers or avoids

350 the cues of benign or noxious prey, respectively. Otherwise, at lower levels of satiation (greater  
351 hunger) the predator is attracted to and consumes previously learned noxious prey. Accordingly,  
352 to forestall starvation it is economically realistic and in agreement with optimal foraging models  
353 for selectivity to decline with decreasing satiation (Houston and McNamara, 1985). At higher  
354 satiation it actively avoids even the stronger appetitive signals. In these behaviors the simulation  
355 agrees with the classic, inverted U-shaped function relating arousal state to performance (Hebb,  
356 1955), and reproduces major behavioral aspects of the real predator (Gillette et al, 2000; Noboa  
357 and Gillette, 2013).

358         The individual contributions of satiation and learning are naturally significant. However,  
359 the importance of their interactions in prey choice is well illustrated (Fig. 4). Without either one  
360 of satiation and learning, the unrestrained virtual predator takes in great quantities of either prey.  
361 This can be maladaptive to a real predator, where taking more high-quality prey than safely  
362 handled by digestion is physiologically threatening. Satiation limits the number of prey taken,  
363 but without learning noxious prey species are taken indiscriminately. Learning prey values  
364 promotes specific exploitation of the benign species and reduces attempts on the noxious species  
365 to periods of near-starvation, when a potential small benefit could be important to survival.

366         In Cyberslug, as in *Pleurobranchaea*, appetitive state is the continuous integration of  
367 sensation, internal state, and memory, and it sets the thresholds for expressing goal-directed  
368 behavior. Cyberslug summates the variables as appetitive state in the core Equation 6 to yield  
369 output that can switch avoidance responses to approach. Sensory integration in the model  
370 accomplishes two critical actions: evaluating the sensory stimuli as *Incentive*, and providing a  
371 spatial map of stimulus location. Thus, *Incentive* sums the primary odor nutritional signal

372 (betaine) with positive and negative qualities learned from previous encounters with the initially  
373 neutral, specific odor signatures of its prey (Eq. 4.1).

374 In the absence of incentive input to the feeding network, appetitive state is solely  
375 dependent on the motivational variable satiation. However, with incentivized sensory input  
376 appetitive state becomes equivalent to “incentive salience” as defined in rodents and primates  
377 (Berridge and Robinson, 2016), where goal-oriented desire becomes tightly linked to reward  
378 cues and is critical to establishing preferences. The fuller concept of “motivational salience”  
379 regulating the attraction or aversion to objects in mammals (Puglisi-Allegra and Ventura, 2016)  
380 emerges in the present model with regulation of the approach-avoidance switch by appetitive  
381 state. Thus the model illustrates how the salience of a stimulus may interact with motivational  
382 state and learning to determine its attractiveness or aversiveness.

383 Stimulus mapping is analogous to that done in the peripheral nervous system of the  
384 animal’s oral veil (Yafremava and Gillette, 2011): a virtual place code represents the averaged  
385 location of an odor stimulus as *Somatic\_Map*, and incorporates an analog of lateral inhibition as  
386 seen in the animal (Eq. 3.1). This provides a template to map the motor output of the turn angle  
387 response, much like functions of superior colliculus and cortex in vertebrates.

388 Cyberslug implements essential elements of an affectively controlled, primitive type of  
389 immediate (or “anoetic”, unknowing) consciousness (Tulving, 1985) whose experience is largely  
390 a moment-to-moment event. It is a rudimentary form postulated as an evolutionary precursor to  
391 higher conscious functions of self-awareness in contexts of semantic and episodic memory  
392 (Tulving, 1985; Denton, 1999; Vandekerckhove and Panksepp, 2011; Vandekerckhove et al.,  
393 2014). In more complex animals, the simple immediate consciousness persists in the subpallial  
394 mechanisms that generate motivation and reward to drive homeostatic behavior, and which

395 thereby sustain and direct the higher cognitive functions (Vandekerckhove and Panksepp, 2011).  
396 The rules governing choice in *Pleurobranchaea* and Cyberslug may resemble a core type of  
397 decision module present in ancestors of the major bilaterian lineages, before the evolution of the  
398 complex brains and behaviors that accompanied segmentation, articulated skeletons, and greater  
399 behavioral involvement in reproduction (Gillette and Brown, 2015). In the vertebrates, control of  
400 approach-avoidance decision is a basic function of the basal ganglia and hypothalamus. In  
401 arthropod nervous systems, these functions are performed by antennal lobes and mushroom  
402 bodies, which may conserve homologous structures as well as analogous functions (Strausfeld  
403 and Hirth, 2013). The feeding network in *Pleurobranchaea* combines functions of vertebrate  
404 hypothalamus and basal ganglia for motivation, incentive comparison, and selection of motor  
405 actions. The more complicated and modularized circuitries in vertebrates and arthropods reflect  
406 more complex bodies and lifestyles, but their brains were likely built onto a basic structure as  
407 shown here.

408         Little previous evidence has been found for empirically driven neuroeconomic  
409 simulations such as this one. However, it is notable that the innovative 1996 videogame  
410 *Creatures* used a bottom-up approach to AI character development, combining basic concepts of  
411 motivation and drive with Hebbian-like learning mechanisms in large artificial neural networks  
412 to achieve interesting behavior. This simulation is designed for transparency and interactivenss.  
413 Users may discover diverse, and perhaps unexpected, emergent properties for forager decision  
414 and prey vulnerability by altering their densities, particularly with the Batesian mimic, and by  
415 altering properties in the code.

416         The simple relations on which Cyberslug runs are readily adaptable to faster-executing  
417 computer languages, fine graphics, artificial neural networks, and neuromorphic representations.

418 The present simple presentation of Cyberslug's behavior in real-time is intended to offer ready  
419 accessibility to a broad audience. The core decision module is open to practical improvements in  
420 learning algorithms, including addition of mechanisms for behavioral habituation and  
421 sensitization. More potential is present; for instance, the model embodies an essential character  
422 of the addictive process in incentivization, and might with little modification reproduce the  
423 sequelae of addiction, withdrawal, and cravings.

424         The homeostatic circuit relations underlying hunger drive in Cyberslug and  
425 *Pleurobranchaea* are adaptable to acquiring other resource types, such as hydration, salt balance,  
426 shelter, play, and social interactions, to name a notable few common to vertebrates. Truly  
427 intelligent and sentient virtual entities, defined in terms of empathic communication and abstract  
428 thought, may not yet exist because they lack the constellation of autonomy, motivation,  
429 valuation, emotion, and social awareness (cf. also Minsky, 2006). Of these, Cyberslug supplies  
430 essential aspects of autonomy, biologically based motivation, and valence assignment. It is  
431 reasonable that cognitive and social features might be added in simple piecemeal fashion  
432 following an evolutionarily plausible course, guided by comparative reference to invertebrate  
433 and vertebrate species that vary incrementally in their cognitive and social expressions with  
434 complexity of lifestyle. Of necessity in evolution, most valuation and decision processes in the  
435 economies of complex social animals would have been elaborated onto pre-existing, simpler  
436 decision modules for homeostasis, like those of *Pleurobranchaea* and other simple invertebrate  
437 foragers. The present relations are similarly open to embellishment in simulation.

438

439 **References**

- 440 Berridge KC, Robinson TE. Liking, wanting, and the incentive-sensitization theory of addiction.  
441 Amer Psychol 2016;71(8):670.
- 442 Boehler C, Tsotsos J, Schoenfeld M, Heinze H-J, Hopf J-M. The center-surround profile of the  
443 focus of attention arises from recurrent processing in visual cortex. Cerebral Cortex.  
444 2008;19(4):982-91.
- 445 Brown JW. Reciprocal interactions between feeding and turning motor networks mediate  
446 foraging decisions in a predatory sea-slug: PhD thesis, University of Illinois at Urbana-  
447 Champaign; 2014.
- 448 Danks D. Equilibria of the Rescorla–Wagner model. J Math Psychol 2003;47(2):109-21.
- 449 Davis W, Villet J, Lee D, Rigler M, Gillette R, Prince E. Selective and differential avoidance  
450 learning in the feeding and withdrawal behavior of *Pleurobranchaea californica*. J Comp  
451 Physiol A: Neuroethology, Sensory, Neural, and Behavioral Physiology. 1980;138(2):157-65.
- 452 Davis WJ, Gillette R. Neural correlate of behavioral plasticity in command neurons of  
453 *Pleurobranchaea*. Science. 1978;199(4330):801-4.
- 454 Denton D, Shade R, Zamariippa F, Egan G, Blair-West J, McKinley M, et al. Neuroimaging of  
455 genesis and satiation of thirst and an interoceptor-driven theory of origins of primary  
456 consciousness. Proc Nat Acad Sci. 1999;96(9):5304-9.
- 457 Gillette R, Brown JW. The sea slug, *Pleurobranchaea californica*: A signpost species in the  
458 evolution of complex nervous systems and behavior. Integ Comp Biol 2015;55(6):1058-69.

- 459 Gillette R, Huang R-C, Hatcher N, Moroz LL. Cost-benefit analysis potential in feeding behavior  
460 of a predatory snail by integration of hunger, taste, and pain. Proc Natl Acad Sci  
461 2000;97(7):3585-90.
- 462 Gillette R, Kovac MP, Davis W. Control of feeding motor output by paracerebral neurons in  
463 brain of *Pleurobranchaea californica*. J Neurophysiol 1982;47(5):885-908.
- 464 Hebb DO. Drives and the CNS (conceptual nervous system). Psychol Rev 1955;62(4):243.
- 465 Hirayama K, Catanho M, Brown JW, Gillette R. A core circuit module for cost/benefit decision.  
466 Frontiers Neurosci. 2012;6.
- 467 Hirayama K, Gillette R. A neuronal network switch for approach/avoidance toggled by  
468 appetitive state. Curr Biol. 2012;22(2):118-23.
- 469 Hirayama K, Moroz LL, Hatcher NG, Gillette R. Neuromodulatory control of a goal-directed  
470 decision. PloS One. 2014;9(7):e102240.
- 471 Houston A, McNamara J. The choice of two prey types that minimises the probability of  
472 starvation. Behav Ecol Sociobiol. 1985;17(2), 135-141.
- 473 Jing J, Gillette R. Directional avoidance turns encoded by single interneurons and sustained by  
474 multifunctional serotonergic cells. J Neurosci. 2003;23(7):3039-51.
- 475 Jing J, Gillette R. Escape swim network interneurons have diverse roles in behavioral switching  
476 and putative arousal in *Pleurobranchaea*. J Neurophysiol 2000;83(3):1346-55.
- 477 London JA, Gillette R. Mechanism for food avoidance learning in the central pattern generator of  
478 feeding behavior of *Pleurobranchaea californica*. Proc Natl Acad Sci 1986;83(11):4058-62.



- 479 Miller RR, Barnet RC, Grahame NJ. Assessment of the Rescorla-Wagner model. Psychol Bull  
480 1995;117(3):363.
- 481 Minsky M. The emotion machine. New York: Pantheon. 2006;56.  
482
- 483 Mpitsos GJ, Cohan CS. Differential Pavlovian conditioning in the mollusc *Pleurobranchaea*.  
484 Devel Neurobiol. 1986;17(5):487-97.
- 485 Mpitsos GJ, Cohan CS. Discriminative behavior and Pavlovian conditioning in the mollusc  
486 *Pleurobranchaea*. Devel Neurobiol 1986;17(5):469-86.
- 487 Noboa V, Gillette R. Selective prey avoidance learning in the predatory sea slug  
488 *Pleurobranchaea californica*. J Exp Biol 2013;216(17):3231-6.
- 489 Puglisi-Allegra S, Ventura R. Prefrontal/accumbal catecholamine system processes high  
490 motivational salience. Frontiers Behav Neurosci. 2012;6.
- 491 Rasmussen A, Zucca R, Johansson F, Jirenhed D-A, Hesslow G. Purkinje cell activity during  
492 classical conditioning with different conditional stimuli explains central tenet of Rescorla-  
493 Wagner model. Proc Natl Acad Sci 2015;112(45):14060-5.
- 494 Rescorla RA, Wagner AR. A theory of Pavlovian conditioning: variations in the effectiveness of  
495 reinforcement and nonreinforcement. In: Black AH, Prokasy WF, editors. Classical Conditioning  
496 II: Current Research and Theory. New York: Appleton-Century-Crofts; 1972. P. 64-99.
- 497 Strausfeld NJ, Hirth F. Deep homology of arthropod central complex and vertebrate basal  
498 ganglia. Science. 2013;340(6129):157-61.
- 499 Tulving E. Memory and consciousness. Canadian Psychol 1985;26(1):1.

500 Vandekerckhove M, Bulnes LC, Panksepp J. The emergence of primary anoetic consciousness in  
501 episodic memory. *Frontiers Behav Neurosci* 2014;7:210.

502 Vandekerckhove M, Panksepp J. A neurocognitive theory of higher mental emergence: From  
503 anoetic affective experiences to noetic knowledge and auto-noetic awareness. *Neurosci Biobehav*  
504 *Rev* 2011;35(9):2017-25.

505 Wilensky U. NetLogo: Center for connected learning and computer-based modeling.  
506 Northwestern University, Evanston, IL. 1999;4952.

507 Yafremava LS, Anthony CW, Lane L, Campbell JK, Gillette R Orienting and avoidance turning  
508 are precisely computed by the predatory sea-slug *Pleurobranchaea californica* McFarland. *J Exp*  
509 *Biol.* 2007;210(4):561-9.

510 Yafremava LS, Gillette R Putative lateral inhibition in sensory processing for directional turns. *J*  
511 *Neurophysiol.* 2011;105(6):2885-90.

512

513 **Figure Legends:**

514 **Fig. 1. Approach-avoidance modeling in *Pleurobranchaea*.** Appetitive State (excitation of the  
515 feeding network) summates intrinsic and learned stimulus values (Incentive) with satiety to  
516 regulate turn response direction. In parallel, a somatotopic map of a stimulus in the animal's oral  
517 veil sets the turn trajectory. Incentive sums sensory inputs predicting intrinsic nutritional value  
518 (Resource Signal) and the learned positive and negative values of prey odor signatures (R+ and  
519 R-). The positive or negative consequences of attacking the different prey are learned through  
520 instructive feedback from the Feeding Network. In the absence of Incentive, basal Appetitive  
521 state simply represents the animal's satiation state (a negative feedback from prey capture). At

522 some threshold, Feeding Network outputs change the turn motor response to a stimulus from  
523 default avoidance to an approach turn. A sensory place code (Somatic Map) for stimuli provides  
524 a template for turn response amplitude in both approach and avoidance. Negative feedback to the  
525 Feeding Network from the Turn Network during avoidance transiently suppresses feeding, while  
526 Feeding Network activity is reduced as Satiation increases. The model is modified from refs. 7  
527 and 8.

528

529 **Fig. 2. Logical flow in the Cyberslug model.** Sensory inputs (SNS) for resource signal odor  
530 (Bet) and learned values of prey odor signatures (Flab and Hermi) are integrated into Incentive  
531 and summate with Satiation in appetitive state (App\_State). Sensory somatotopic place  
532 information is encoded in Somatic Map, which acts as a template for the turn response  
533 amplitude. The turn motor network (TN) responds by default to sensory input with an avoidance  
534 turn response unless input from App\_State is high enough to switch the turn to approach; this is  
535 mediated directly by a simple dyadic disinhibitory switch ( $ASw_{1,2}$ ). Successful predation  
536 increases satiation which in return reduces App\_State.

537

538 **Fig. 3. Screenshots of the Cyberslug environment and interface.** Frames are shown from  
539 early (upper) and later (lower) in a software run. The Cyberslug agent (orange) encounters Hermi  
540 (green orbs) and Flab (red orbs) in its environment and traces its path (orange contours). Users  
541 can select the number of prey in the environment, move Cyberslug manually, or toggle the path  
542 tracer. Various Cyberslug and environmental parameters are updated in real-time, as shown. In  
543 the early frame the Cyberslug is orienting toward prey (App\_State = 0.545, high;

544 App\_State\_Switch = -1), and in the later frame it is in aversive mode (App\_State = 0.029, low;

545 App\_State\_Switch = +1).

546

547 **Fig. 4. Effects of learning and satiation, and their interactions, on prey selectivity and total**

548 **prey consumed.** Without either mechanism for learning or satiation, selectivity was low and

549 prey were consumed as encountered in the 10 Flab/3 Hermi arena. Adding learning mechanisms

550 did not alter either selectivity or number of prey consumed. When satiation was present without

551 learning, prey consumed dropped but selectivity was unchanged. When both learning and

552 satiation mechanisms operated, selectivity was high and total prey consumed dropped to even

553 lower values (One-way ANOVA across the four behavioral scenarios,  $p < 0.0001$ . \*\*\*  $p < 0.001$

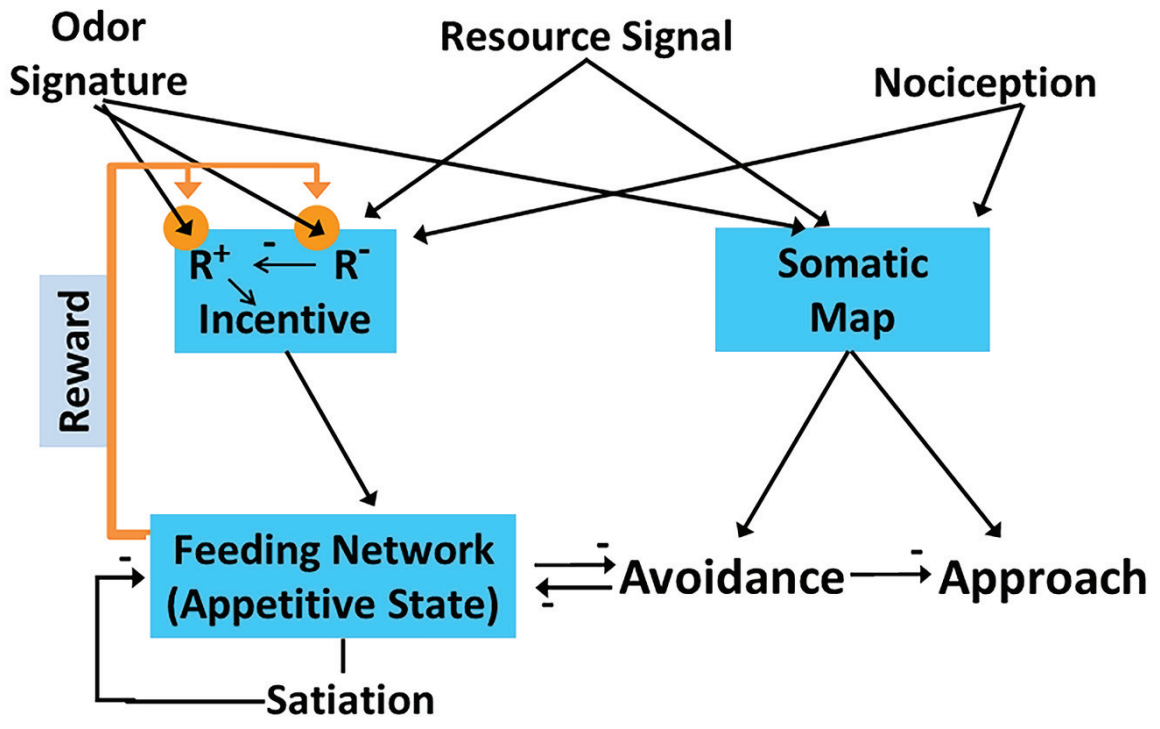
554 relative to all other learning/satiation scenarios (Tukey-Kramer,  $n=6$  trials in each)). Differences

555 in selectivity between the first three learning/satiation scenarios, or in prey consumption where

556 satiation was inactivated, were not significant ( $p > 0.05$ ) Error bars are standard errors of the

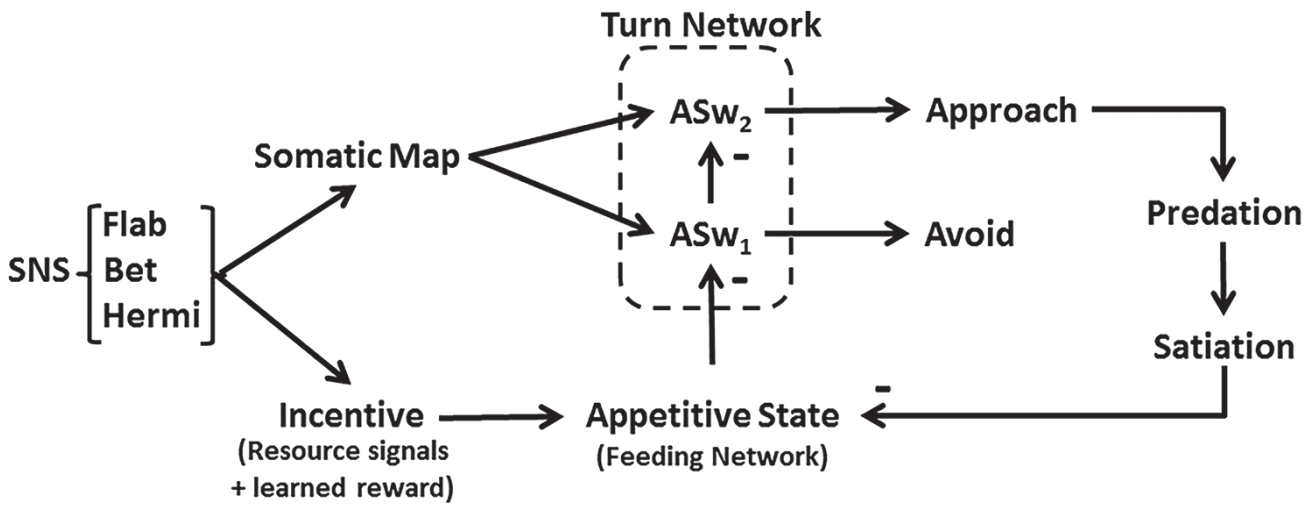
557 mean. See text for further explanation.

558



Synapses modifiable by learning ●

Feedback potentiation of Hebbian learning →



setup go

step

hermi-populate 3

flab-populate 10

fauxflab-populate 0

Bet-L 4.68 Bet-R 4.45

Hermi-L 2.82 Hermi-R 2.01

Flab-L 4.67 Flab-R 4.45

sns\_betaine 4.56

sns\_hermi 2.42 sns\_flab 2.42

show-sensors



V\_Hermi (Learning) 0

V\_Flab (Learning) 0

App\_State 0.69

App\_State\_Switch -1

Incentive Sallence 4.8

Somatic\_Map -0.23

Hermisenda eaten 0

Flabellina eaten 0

Faux-Flabellina eaten 0

Nutrition 0.31

Satiation 0.16

Reward 4.8

Reward-neg 0

setup go

step

hermi-populate 3

flab-populate 10

fauxflab-populate 0

Bet-L 2.63 Bet-R 2.52

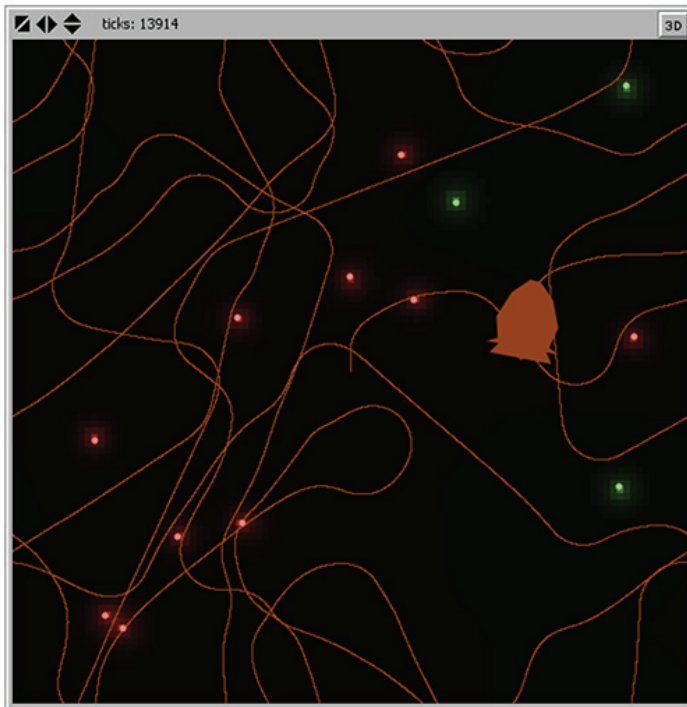
Hermi-L 0.5 Hermi-R 0.19

Flab-L 2.62 Flab-R 2.52

sns\_betaine 2.57

sns\_hermi 0.35 sns\_flab 0.35

show-sensors



V\_Hermi (Learning) 0.984

V\_Flab (Learning) 0.875

App\_State 0.13

App\_State\_Switch 1

Incentive Sallence -0.24

Somatic\_Map -0.11

Hermisenda eaten 6

Flabellina eaten 3

Faux-Flabellina eaten 0

Nutrition 0.35

Satiation 0.19

Reward 2.73

Reward-neg 2.97

